Kovove Mater. 51 2013 37–44
DOI: 10.4149/km_2013_1_37

Numerical simulation and experimental analysis of simultaneous melting and burnishing of 304 stainless steel with oscillatory laser heat source

T. Moscicki*, J. Radziejewska

Institute of Fundamental Technological Research, Polish Academy of Sciences, ul. Pawinskiego 5B, 02-106 Warszawa, Poland

Received 4 July 2012, received in revised form 13 September 2012, accepted 20 September 2012

Abstract

In this paper the simultaneous laser melting and burnishing of a stainless steel is studied both experimentally and theoretically. A continuous CO_2 laser beam is moving either along a straight line or criss-crossing it. It has been shown that the oscillatory movement of the laser source together with the burnishing results in a better surface topography comparing to the non-oscillatory process. A theoretical modelling is applied to calculate the temperature field during the process. The results of theoretical analysis are verified by analyzing microstructure changes of the material in laser heated zone. It has been found that a very good agreement between theoretical and experimental results is achieved when the change of the absorptivity of the laser beam with the temperature of the melted zone is taken into account.

K e y w o r d s: laser treatment, hybrid treatment, surface structure, mathematical modelling

1. Introduction

Laser Beam Machining (LBM) has been successfully applied for improvement of surface layer properties. The advantages of LBM are: high speed machining, a possibility of performing the process in open atmosphere, the modification of freely selected small fragments of the surface as well as the savings on the costs of material. The disadvantages of the LBM are the relatively high roughness of the surface after the process and tensile stresses in melted layer [1, 2]. In practice an abrasive machining of the surface is performed after LBM. However, it results in the removal of some volume of the formed layers, which reduces the positive effects of the LBM.

In [3] a new method of modification of the surface layer, combing the laser melting with the slide burnishing, was proposed. The smoothing of surface was carried out by plastic deformation of surface layer at high temperature, whereas transformation process of stresses, from tensile to compressive stresses, was performed by plastic deformation at low temperatures. All operations, high and low temperature burnishing, were performed simultaneously on the laser station, in one pass. The temperature distribution in the burnishing zone was determined initially on the basis of the analytic solution, where a moving source of heat with a Gaussian distribution of energy density was considered. The distribution in a half-space had an approximate character because of numerous simplified assumptions [4]. The results of the calculations were shown in work [3].

The high degree of strain hardening of surface and thickness of strained hardening zone up to 0.3 mm was obtained using micro-hammering combined with laser alloying [5]. The problem was a formation of grooves in hot plastic materials. In order to obtain more uniform deformation of surface material, the oscillatory, sinusoidal motion of the sample in a direction perpendicular to the direction of feed speed was introduced. The motion was generated using an oscillating table. The oscillatory motion eliminated the problem of the formation of unfavourable surface texture but also influenced the temperature distribution in the burnishing area and the shape of the melting zone. The knowledge of the temperature distribution in the burnish-

*Corresponding author: e-mail address: tmosc@ippt.gov.pl

ing zone and the shape of melted zone are necessary to determine optimum parameters of the burnishing process. It enables selection of micro-hammers impact forces to obtain a suitably strain hardening thick zone of the treated surface and guarantees the compressive stresses in the whole melting zone. Thus it provides favourable operating properties, especially in terms of fatigue [6].

The current work presents the analysis of the temperature distribution in the burnishing area. A new theoretical model of the oscillating laser source was used to calculate the temperature field in the area of stainless steel heated with a continuous CO_2 laser. The hydrodynamic model of laser beam interaction with metallic surface has been improved since the sixties [7]. Unfortunately, the differences between experimental results and theoretical modelling are still significant and need further investigation. In the last years an emphasis was put on taking into account the realistic shape of the laser beam intensity distribution [8], the turbulent flow in the melted zone [9, 10], or the changes of surface tension in boundary condition [9, 11]. However, none of publications that considered modelling of melting process took into account the oscillatory movement of the laser source or changes of the absorptivity after melting of material. In addition, even in the recent publications which considered laser machining with a phase transformation, a constant absorptivity was assumed [8, 9, 12]. In many cases the reflectivity of metal is so strong that a surface coating such as colloidal graphite is applied to improve absorption of the laser light. During interaction of the laser beam with the surface, graphite coating vanishes from the surface due to burning and intensive flow in the molten zone. This causes the absorptivity decrease and the surface reflectivity increase [13]. On the other hand, the change of phase from solid to liquid results in the absorptivity increase. The calculation of the Fresnel absorption indicates the rise in absorption from 6 % for solid to 14 % for liquid iron [14]. (Additionally, in the case of deep penetration that takes place during keyhole welding, the absorption of the laser beam reaches $\sim$ 100 % as a result of increasing the angle of incidence and multiple reflections inside the keyhole.)

The simplified models leave some questions unanswered. In particular there is no explanation why at certain speed rate the volume of melted material unexpectedly increases. In this paper the analysis of the laser melting of stainless steel at different speed rates with and without oscillatory movement of the laser beam was made. In order to improve accuracy of the theoretical calculations the change of the absorptivity with the melting temperature as well as the real power distribution of the laser beam was taken into account. The results of theoretical analysis have been verified by comparison with the experimental results. The size and shape of the melting zone were obtained from the analysis of the microstructure changes of the material.

2. The experiment description

2.1. Laser-mechanical treatment

The study was performed using the CO_2 laser with the maximum power 2.5 kW. The axially-symmetric beam, of the mode close to TEM10, was focused with use of the ZnSe lens. The focal length of it was 5". The melting was carried out on steel 304 at laser power 2 kW, laser beam diameter of 2.6 mm, feed rate of sample against the laser beam from 150 to 900 mm min^{-1}.

The burnishing process was carried on the laser station simultaneously with the melting process. The dynamic burnishing process with use of a head with micro-hammers was applied. The technology of micro-hammering was based on a dynamic centrifugal burnishing. Processing concept and principle of operation of the head is described in [5]. Two rows of 8 micro-

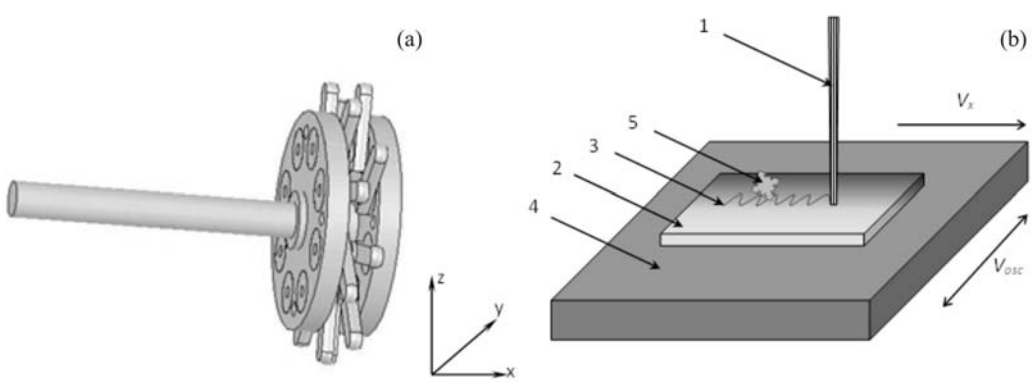

Fig. 1. a – dynamic burnishing head, b – scheme of the station for laser-mechanical treatment: 1 – laser beam, 2 – sample, 3 – laser path, 4 – oscillation table, 5 – dynamic burnishing head.

-hammers enable the simultaneous burnishing of two regions with different temperatures. In order to obtain more uniform deformation of the surface material the oscillatory motion of the sample in a direction perpendicular to the direction of feed rate was introduced. The motion was generated using an oscillating table. The oscillation eliminated the problem of formation of the grooves – an unfavourable surface geometric structure. A constant velocity 15.5 oscillations per second and the amplitude of 1.2 mm were used. The small radii of micro-hammers allow obtaining high surface plastic deformation at low forces. The scheme of the head is shown in Fig. 1a while the laser-mechanical treatment is presented in Fig. 1b.

2.2. Mathematical analysis for laser heating with phase change

The transient model which describes the re-melting of stainless steel with and without an oscillatory movement was solved for 3D geometry with the use of commercially available Ansys-Fluent software package [15, 16]. It has been assumed that the laser beam moves with velocity v and interacts with a sample of finite dimensions. The laser beam was focused on the surface with diameter $w_0 = 2.6$ mm and the laser power P was 2 kW. The set of equations used by Ansys-Fluent consists of equations of conservation of mass, energy and the momentum equation in the form:

$$\frac{\partial \rho}{\partial t} + \nabla \cdot (\rho \vec{v}) = 0, \tag{1}$$

$$\frac{\partial}{\partial t}(\rho E) + \nabla \cdot (\vec{v}(\rho E + p)) = \nabla \cdot \left(k \nabla T + \overline{\overline{\tau}}_{\text{eff}} \cdot \vec{v}\right) + S_{\text{h}}, \tag{2}$$

$$\frac{\partial}{\partial t}(\rho \vec{v}) + \nabla \cdot (\rho \vec{v}\vec{v}) = -\nabla p + \nabla \cdot \left(\overline{\overline{\tau}}\right) + \rho \vec{g} + \vec{F}, \tag{3}$$

where $\overline{\overline{\tau}}$ is the viscous tensor,

$$\overline{\overline{\tau}} = \mu \left[\left(\nabla \vec{v} + \nabla \vec{v}^{\text{T}} \right) - \frac{2}{3} \nabla \cdot \vec{v} I \right], \tag{4}$$

E is energy, $E = h - p/\rho + 0.5v^2$, h is enthalpy, $h = \int_{T_0}^{T} c_{\text{p}} \text{d}T + f_{\text{l}} L_{\text{m}}$, where c_{p} is the specific heat at constant pressure, L_{m} is the latent heat of melting. The liquid fraction f_{l} is defined as 0 for $T < T_{\text{sol}}$, 1 for $T_{\text{liq}} < T$ and $f_{\text{l}} = \dfrac{T - T_{\text{sol}}}{T_{\text{liq}} - T_{\text{sol}}}$ if $T_{\text{sol}} < T < T_{\text{liq}}$. T_{sol} and T_{liq} denote solidus and liquidus temperature, respectively, ρ is the mass density, p is the pressure, $\vec{v}$ is the velocity vector, k is the thermal conductivity, T is the temperature, S_{h} is the internal heat source, $\vec{g}$ is the gravity, $\vec{F}$ is the external force, μ is the dynamic viscosity, I is the unit tensor.

In addition, the model must include the partial differential equations describing the turbulence in the re-melted zone:

$$\frac{\partial}{\partial t}(\rho K) + \nabla \cdot (\rho K \vec{v}) = \\ = \nabla \cdot \left[\left(\mu + \frac{\mu_{\text{t}}}{\sigma_{\text{K}}} \right) \nabla K \right] + G_{\text{K}} - \rho \varepsilon, \tag{5}$$

$$\frac{\partial}{\partial t}(\rho \varepsilon) + \nabla \cdot (\rho \varepsilon \vec{v}) = \\ = \nabla \cdot \left[\left(\mu + \frac{\mu_{\text{t}}}{\sigma_{\varepsilon}} \right) \nabla \varepsilon \right] + C_1 \frac{\varepsilon}{K} G_{\text{K}} - C_2 \rho \frac{\varepsilon^2}{K}. \tag{6}$$

In these equations, G_{K} represents the generation of turbulence kinetic energy due to the mean velocity gradients, C_1, C_2 are constants. σ_{K} and σ_{ε} are the turbulent Prandtl numbers for K – the turbulence kinetic energy and ε – rate of dissipation, respectively. The turbulent viscosity μ_{t} is computed by combining K and ε as follows: $\mu_{\text{t}} = \rho C_{\mu} K^2/\varepsilon$, where C_{μ} is constant [16].

The boundary condition at the place where the laser beam interacts with the surface is:

$$-k \frac{\partial T_{\text{s}}}{\partial \vec{n}} = I_{\text{L}} A - \alpha (T - T_0) - \sigma R \left(T^4 - T_0^4 \right) - \rho u(t) L_{\text{v}}, \tag{7}$$

where I_{L} is the laser intensity, A is the surface absorptivity, α is the coefficient of heat input on the sample surface, σ is the Stefan-Boltzmann constant, T_0 is the ambient temperature, R is the emissivity, L_{v} is the latent heat of vaporization, and $\vec{n}$ is the unit vector perpendicular to the surface.

It can be assumed that the vaporization rate $\rho u(t)$ is given by the Hertz-Knudsen equation and the vapour pressure above the vaporized surface results from the Clausius-Clapeyron equation [15]. Then:

$$u(t) = (1 - \beta) \frac{p_{\text{b}}}{\rho} \left(\frac{m}{2\pi k T_{\text{s}}} \right)^{1/2} \exp \left[\frac{L_{\text{v}}}{k_{\text{B}}} \left(\frac{1}{T_{\text{b}}} - \frac{1}{T_{\text{s}}} \right) \right], \tag{8}$$

where k_{B} is the Boltzmann constant, T_{s} is the surface temperature, T_{b} is the boiling temperature under a reference pressure p_{b}, and β is the fraction of the vaporized particles returning to the target surface (back flux). For stationary vaporization, $\beta = 0.18$.

For the side surfaces of the sample, convection and radiation heat exchange with the surrounding medium was assumed:

$$-k \frac{\partial T_{\text{s}}}{\partial \vec{n}} = -\alpha (T - T_0) - \sigma R \left(T^4 - T_0^4 \right). \tag{9}$$

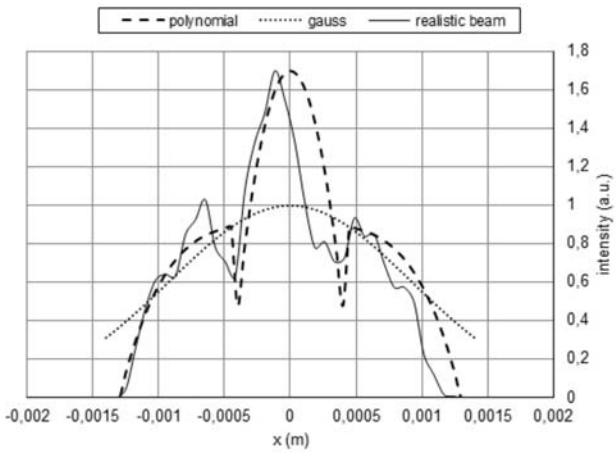

Fig. 2. Fitting of the functions to the realistic laser beam intensity distribution in comparison with the Gaussian distribution.

In the molten zone, where the intermixing of the melted materials takes place, the mass flow is primarily due to the difference in the local surface tension γ. The surface tension stress results from the Marangoni effect and is accounted by the following boundary condition:

$$\tau_{\mathrm{s}} = -\mu\frac{\partial u}{\partial z} = \frac{\partial \gamma}{\partial x} = \frac{\partial \gamma}{\partial T}\cdot\frac{\partial T}{\partial x}. \tag{10}$$

The energy source term I_{L} was used in the form, which fits to the shape of the laser pulse used in our laboratory.

$$I_{\mathrm{L}} = \begin{cases} 0 & \text{for } r > r_{\mathrm{f}}, \\ \dfrac{P}{\pi r_{\mathrm{f}}^2}\left(0.9\left(1-\left(\dfrac{r}{r_{\mathrm{f}}}\right)^4\right)+0.8\left(1-\left(\dfrac{4r}{r_{\mathrm{f}}}\right)^2\right)\right) & \text{for } 0 < r < \dfrac{r_{\mathrm{f}}}{4}, \\ \dfrac{P}{\pi r_{\mathrm{f}}^2}0.9\left(1-\left(\dfrac{r}{r_{\mathrm{f}}}\right)^4\right) & \text{for } \dfrac{r_{\mathrm{f}}}{4} < r < r_{\mathrm{f}}, \end{cases} \tag{11}$$

where r_{f} is the radius of the laser beam on the sample surface, $r = \sqrt{(x - x_0 + dx)^2 + (y - y_0)^2}$, where $dx = ut$ and x_0, y_0 are start point coordinates. The shape of the laser beam intensity distribution with fitted function is shown in Fig. 2. For comparison, the Gaussian distribution was also shown. The difference is significant and has influence on results of calculations.

In the present work the calculations and experiments have been performed using the stainless steel 304 sample of finite dimensions $50 \times 40 \times 5\,\mathrm{mm}^3$. The surface of sample was grinded and covered with colloidal graphite. It was assumed that surface absorptivity A below melting temperature of steel with graphite overlay is 0.6 [12, 17, 18] and 0.14 above liquidus temperature. All the material properties depend on the temperature. Thermo-physical properties such as the specific heat c_{p}, the coefficient of thermal conductivity k, the viscosity μ, the density ρ and the surface tension γ for stainless steel were taken from [19]. Other material properties were as follows: the latent heat of melting $L_{\mathrm{m}} = 270 \times 10^3\ \mathrm{J\,kg^{-1}}$, the latent heat of vaporization $L_{\mathrm{v}} = 6.26 \times 10^6\ \mathrm{J\,kg^{-1}}$, the liquidus temperature $T_{\mathrm{liq}} = 1723\,\mathrm{K}$, solidus temperature $T_{\mathrm{sol}} = 1658\,\mathrm{K}$, and the boiling temperature $T_{\mathrm{b}} = 3135\,\mathrm{K}$.

The oscillatory movement of the laser beam was modelled by the introduction of changes in y direction:

$$dy = A_{\mathrm{os}}\sin(2\pi\omega t), \tag{12}$$

where A_{os} is the amplitude and ω the frequency of oscillations. $A_{\mathrm{os}} = 1.2\,\mathrm{mm}$ and $\omega = 15.5\,\mathrm{s^{-1}}$ were used in calculation.

2.3. Testing methods

Microstructure analysis and measurements of a size of the melted zone were performed on an optical microscope at magnifications from 50 to 1000×. The metallographic micro-sections were made in a direction perpendicular to the direction of feed rate.

The surface topography was examined on a scanning profilometer Form Talysurf after laser melting, and hybrid process was performed with different process parameters. Surface roughness measurements were conducted for each track of the laser melting and the laser melting with oscillatory movement was combined with micro-hammering. The roughness measurements were made in central area of the melting path.

3. Results

3.1. The theoretical calculations

The distribution of temperature at the sample surface (x-y plane) and the distribution of liquid phase at the y-z plane after 1 s, for speeds: 150, 360 and 900 mm min^{-1}, are the results of the model. The depth of melting and size of the heat-affected zone in the x direction at the time exceeding 1 s are practically constant.

Figures 3–5 show the temperature distribution at the surface of sample for all speeds of the laser beam scanning with and without oscillatory movement after 1.016 s. In the case when there are no oscillations the maximal temperature is always on the axis of sample. In the case when the oscillations are added, the maximum of temperature follows the laser beam axis and not always overlays the sample axis. Adding of the oscillation has an explicit influence on the temperature distribution above 600 K. The additional move in y dir-

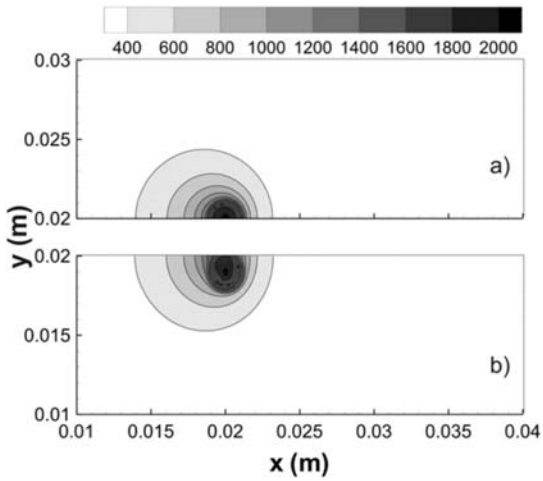

Fig. 3. Temperature distributions at the sample surface. Feed rate 150 mm min^{-1}, time 1.016 s (at outer edge of oscillation); a) without, b) with oscillatory movement.

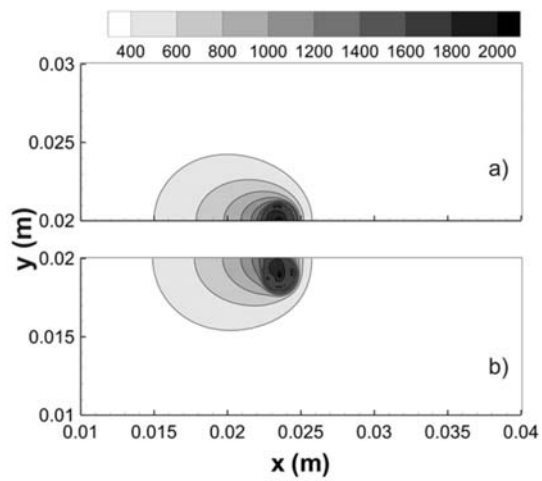

Fig. 4. Temperature distributions at the sample surface. Feed rate 360 mm min^{-1}, time 1.016 s (at outer edge of oscillation); a) without, b) with oscillatory movement.

ection of the laser beam causes almost double increase of the area where the temperature is greater than the melting temperature. The irregular distribution of temperature in the range of 1600–2000 K is caused by realistic shape of laser beam intensity and the change of absorptivity at the liquidus temperature. In the places where the laser beam interacts with the sample at temperature below 1723 K the absorptivity is four times higher than in other regions, what causes a rapid rise of the absorbed energy and hence the temperature increases. This effect is the most pronounced at the higher feed rate. In the region of the first row of micro-hammers, in the distance 5 mm from laser beam, the temperature of the metal surface is

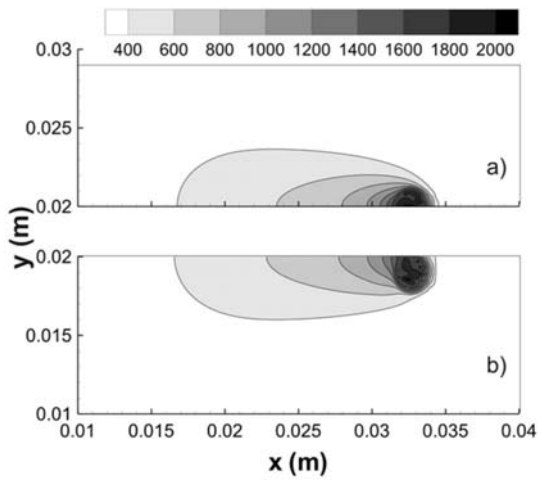

Fig. 5. Temperature distributions at the sample surface. Feed rate 900 mm min^{-1}, time 1.016 s (at outer edge of oscillation); a) without, b) with oscillatory movement.

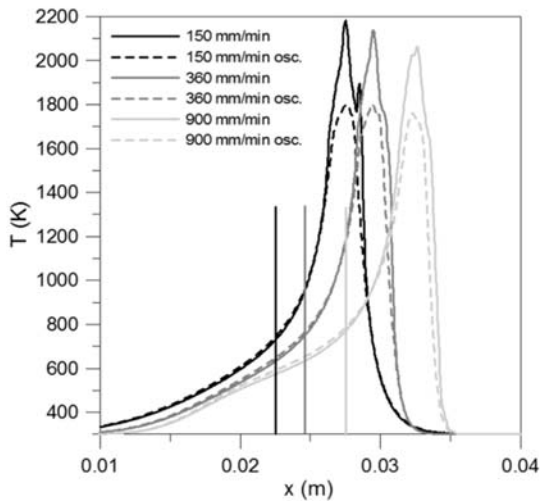

Fig. 6. Calculated distributions of temperature at the material surface along axis x ($y = 0.02$ m) for feed rate 150 after 4 s, 360 after 2 s, and 900 mm min^{-1} after 1 s without (continuous line) and with (dashed line) oscillations. The vertical lines denote distance 5 mm from the laser beam axis.

730 K for feed rate 150 mm min^{-1} and 770 K for 900 mm min^{-1} (Fig. 6).

Application of the oscillatory movement practically does not change the temperature distribution of the burnishing area in comparison to the melting without oscillations. At these temperatures the rise of the plasticity of materials is significant. It allows for the high plastic deformations with use of low impact force of a tool on the material. Higher differences in the temperature distribution at the material surface are in the region of the second row of micro-hammers. In this case the highest temperature for feed rate 900 mm min^{-1}

Table 1. The depth and width of the laser melting zone of 304 stainless steel obtained with different parameters in experiments

V_f (mm min^{-1})	V_{osc} (osc/min)	Amplitude of oscillation (mm)	Depth of melting zone (mm)	Width of melting zone (mm)
900	–		0.424	1.355
360	–		0.605	1.452
150	–		0.791	1.742
900	930	1.2	0.194	3.225
360	930	1.2	0.339	3.267
150	930	1.2	0.531	3.461

Table 2. The depth and width of laser melting zone of 304 stainless steel obtained with different parameters in calculations

V_f (mm min^{-1})	V_{osc} (osc/min)	Amplitude of oscillation (mm)	Depth of melting zone (mm)	Width of melting zone (mm)	Depth of melting zone (mm) $A = 0.22$	Width of melting zone (mm) $A = 0.22$
900	–		0.375	1.32	0.35	0.97
360	–		0.62	1.5	0.76	1.28
150	–		0.78	1.72	0.93	1.44
900	930	1.2	0.16	2.8	0.13	2.02
360	930	1.2	0.36	3.14	0.33	2.44
150	930	1.2	0.52	3.42	0.46	2.52

is 650 K while 550 K for 150 mm min^{-1} on the sample axis.

The model enabled determining the maximal temperature of the process and dimensions of the melting zone. It was assumed that the boundary of the melted zone is in 50 % of liquid fraction for model. The results of the experiment are shown in Table 1 whereas the results of calculations in Table 2.

The comparison of the results for constant and variable absorptivity confirms the adequacy of the assumptions. In the case when absorption is constant (0.22) significant differences between the experimental results and the modelling are observed. The depth of the melted area is in good conformity with the experiment except the case when the highest feed rate (900 mm min^{-1}) has been applied. However, when the width of the melted area is considered the differences are noticeable in all cases. The minimal difference in width is 0.17 mm for 360 mm min^{-1} of feed rate without oscillations and it stands about 12 % compared to the experimental value. The disagreement increases with the rise of the feed rate and it reaches 28.5 % for the speed of 900 mm min^{-1}. When the oscillations are applied, it causes further divergence of the results. In the extreme case (900 mm min^{-1} with oscillations), the difference in width of melted zone is as high as 37.3 %.

Taking into account the change of absorption due to variation of phase state resulted in a good agreement between the theoretical and experimental results. The differences in the dimensions of the depth and width of melting pool do not exceed 10 %. Only for the feed rate of 900 mm min^{-1} with oscillations the difference is higher and can be caused by quality of surface such as unevenness of the steel surface with graphite cover occurring during the experiment. However, the dissimilarity of theoretical and experimental results for this case does not exceed 15 % and shows that the presented model and the adopted input data are correct. Differences in the shape of melting zone in Fig. 7b result from the instantaneous position of the laser beam. In subsequent time steps the beam moves towards the sample axis. This increases the depth of penetration with a simultaneous decrease of the width of melting zone. However, the maximum depth does not change on the axis of sample.

3.2. Experimental investigation

3.2.1. Surface texture

Figure 7 presents the profiles measured perpendicular to the feed direction of samples which underwent: a – laser melting, b – laser melting and micro-hammering, c – laser melting and micro-hammering with oscillations. The distance between the first row of micro-hammers and laser beam axis was 5 mm and rotational speed of micro-hammers head was 7100 rev/min. This allowed obtaining maximum impact force in examined case. The highest temperature in burnishing area was about 750 K. The surface geometrical structure had changed during the burnishing pro-

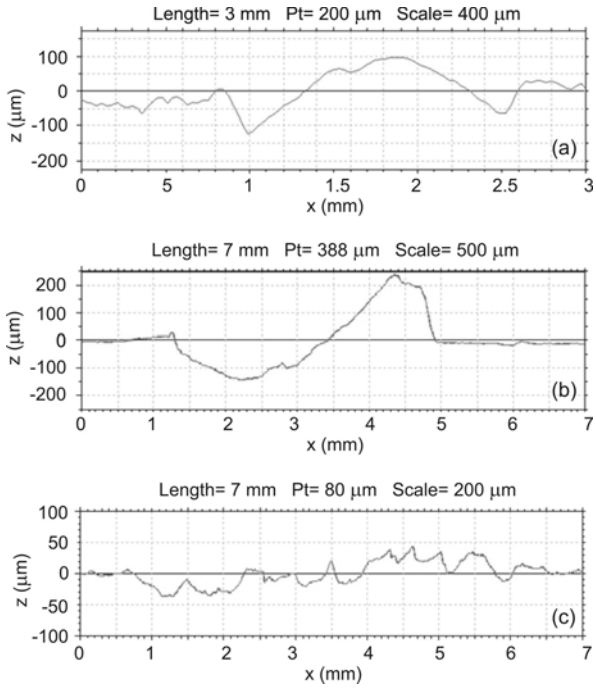

Fig. 7. Profiles of surface after: a – laser melting, b – laser melting and micro-hammering, c – laser melting and micro-hammering with oscillations with amplitude 1.2 mm.

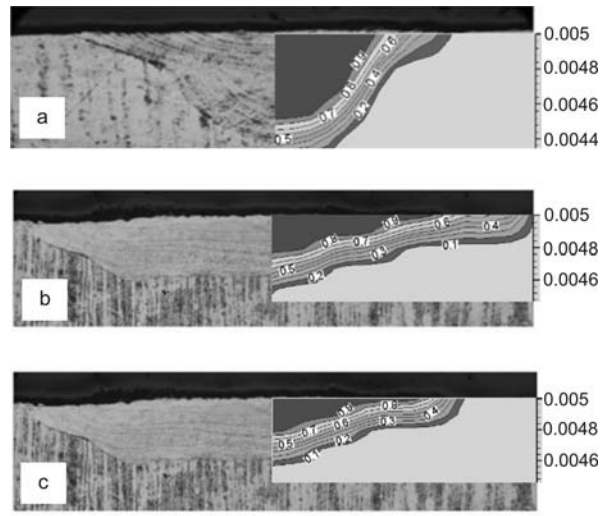

Fig. 8. The shapes of the melted zone (in meter) in direction perpendicular to the feed rate: without oscillations (a), with oscillations (b), and with oscillations at constant absorptivity (c). Feed rate 360 mm min^{-1}. Left – experiment, right – theoretical distribution of the liquid phase.

cess in high temperature. The oscillatory movement in the direction perpendicular to the feed direction allowed eliminating the groove formation. The plastic deformation of surface was more homogeneous. The increase of the width of the treated zone corresponds to the amplitude of the oscillation.

3.2.2. Microstructure of the melting zone

Figure 8a shows the microstructure of surface layer after laser melting with feed speed 360 mm min^{-1} and Fig. 8b presents the microstructure at the same speed with oscillatory movement. The changes of the melting shape connected with oscillation are visible. The width of the melting zone is bigger than the oscillation amplitude. In both cases the capillary lines, parallel to the bottom of melting zone, were disclosed. The right side of the figures presents the theoretical distribution of liquid and solid phase calculated based on the model in which variation of absorption is considered. A good correlation between theoretical and experimental results can be noticed. Worse accuracy has been obtained for constant absorptivity (Fig. 8c).

Table 1 presents the values of width and depth of the melting zone obtained at laser melting at different conditions. The application of the oscillatory movement resulted in an increase of the width melting zone while the melting depth decreased compared to laser melting at the same feed rate without oscillations. The volume of the melted material grows at equal densities of provided energy.

4. Discussion

The study reveals that theoretical analysis of temperature distribution in the area affected by the laser beam shows a good agreement with the experimental results. It can be helpful in the selection of proper parameters of the burnishing process.

The best fit was obtained for the theoretical model which took the real laser power distribution and the change of absorptivity at phase transformation during laser melting into account. In this case, the discrepancy between theoretical and experimental results does not exceed 10 % for the feed speed 150 mm min^{-1} and 360 mm min^{-1}. In case of constant absorptivity the accuracy of the computed temperature results is lower. The study on the depth of laser melting area shows a good agreement of the experimental results whereas when the melting zone width is analyzed significant differences are revealed, especially when the oscillatory movement is considered.

The elaborated theoretical model allows to predict with high accuracy the size of the melting zone as well as the temperature distribution in the burnishing area. Based on the model and the knowledge of changes of mechanical properties due to temperature variation it is possible to select burnishing parameters. The proper temperature, micro-hammers impact force on surface and intensity of the burnishing process provide uniform plastic deformation as well as

the assumed thickness of strained hardening zone. The tensile stresses, which lead in extreme case to cracking of surface layer, can be reduced by properly chosen thickness and degree of the strain hardening.

The oscillatory movement in direction perpendicular to the feed rate results in better surface topography and disappearance of the grooves formation during the burnishing process in high temperature in contrast to the hybrid treatment without oscillations. The highest temperature of surface of the laser heated zone is lower of about 200–400 K and the effectiveness of the melting process is greater than melting without oscillations. At the same energy of the laser beam the volume of melted material is greater in the case of oscillations. This is due to the higher surface absorptivity at lower temperature.

5. Conclusions

It has been shown that the oscillatory movement of the laser source together with the burnishing results in better surface topography as well as in more homogeneous plastic deformation of the surface comparing to the non-oscillatory process. The experimentally and theoretically obtained shapes of the melted zone are in good agreement. This shows that the theoretical model of melting which takes into account the absorptivity change with the phase transformation accurately determines the temperature distribution in the heated zone. In particular it explains the increase of the volume of melted material in the case of oscillations movement. The effectiveness of laser surface melting is the highest for melting with oscillating heat source; this technical solution can be applied in other fields of laser processing.

References

[1] Mejer, J.: J. of Material Processing Technology, *149*, 2004, p. 2. doi:10.1016/j.jmatprotec.2004.02.003
[2] Kovalenko, V. S.: Components Hardening with Laser Beam. Kijev, Technika 1981.
[3] Anthony, T. R., Cline, H. E.: J. Appl. Phys., *48*, 1977, p. 1767.
[4] Radziejewska, J., Skrzypek, S. J.: J. of Materials Processing Technology, *209*, 2009, p. 2047. doi:10.1016/j.jmatprotec.2008.04.067
[5] Radziejewska, J.: Materials and Design, *32*, 2011, p. 5073. doi:10.1016/j.matdes.2011.06.035
[6] Przybylski, W.: Burnishing Technique. Warsaw, PWN 1981.
[7] Akbari, M., Sinton, D., Bahrami, M.: Journal of Heat Transfer, *133*, 064502, 2011. doi:10.1115/1.4003155
[8] Momin, O., Shuja, S. Z., Yilbas, B. S.: Optics & Laser Technology, *44*, 2012, p. 463. doi:10.1016/j.optlastec.2011.08.014
[9] Didenko, T., Kusinski, J., Kusinski, G.: AIP Conf. Proc., *973*, 2008, p. 640. doi:10.1063/1.2896855
[10] Charabotrty, N.: App. Thermal Eng., *29*, 2009, p. 3618. doi:10.1016/j.applthermaleng.2009.06.018
[11] Chan, C. L., Mazumder, J., Chen, M. M.: J. Appl. Phys., *64*, 1988, p. 6166. doi:10.1063/1.342121
[12] Xu, H., Chen, W. W., Zhou, K., Huang, Y., Wang, Q. J.: Int. J. Adv. Manuf. Technol., *47*, 2010, p. 679. doi:10.1007/s00170-009-2206-5
[13] Engel, S. L.: Source Book on Applications of the Laser in Metalworking. Ed.: Metzbower, E. A. Metals Park, American Society for Metals 1981, p. 149.
[14] Hoffman, J., Szymański, Z.: Optica Applicata, *32*, 2002, p. 129.
[15] Moscicki, T., Hoffman, J., Szymanski, Z.: Arch. Mech., *63*, 2011, p. 99.
[16] Ansys FLUENT 12.0/12.1 Documentation.
[17] Hoffman, J.: J. Tech. Phys., *36*, 1995, p. 11.
[18] Courtney, C., Stehen, W. M.: In: Proc. of Int. Conf. on Advances in Surface Coatings Technology. Ed.: Anderson, J. C. Cambridge, UK, British Welding Institute 1978, p. 219.
[19] Mills, K. C.: Recommended Values of Thermophysical Properties for Selected Commercial Alloys. Cambridge, UK, Woodhead Publishing Limited 2012.